Structural Engineering and Mechanics, Vol. 24, No. 4 (2006) 395-410

DOI: http://dx.doi.org/10.12989/sem.2006.24.4.395

Wave propagation in laminated piezoelectric cylindrical shells in hydrothermal environment

K. Dong† and X. Wang‡

Department of Engineering Mechanics, School of Naval Architecture, Ocean and Civil Engineering, Shanghai Jiao Tong University, Shanghai 200030, P. R. China

(Received July 5, 2005, Accepted June 15, 2006)

Abstract. This paper reports the result of an investigation into wave propagation in orthotropic laminated piezoelectric cylindrical shells in hydrothermal environment. A dynamic model of laminated piezoelectric cylindrical shell is derived based on Cooper-Naghdi shell theory considering the effects of transverse shear and rotary inertia. The wave characteristics curves are obtained by solving an eigenvalue problem. The effects of layer numbers, thickness of piezoelectric layers, thermal loads and humid loads on the wave characteristics curves are discussed through numerical results. The solving method presented in the paper is validated by the solution of a classical elastic shell non-containing the effects of transverse shear and rotary inertia. The new features of the wave propagation in laminated piezoelectric cylindrical shells with various laminated material, layer numbers and thickness in hydrothermal environment and some meaningful and interesting results in this paper are helpful for the application and the design of the ultrasonic inspection techniques and structural health monitoring.

Keywords: laminated piezoelectric cylindrical shells; wave characteristics curves; transverse shear and rotary inertia; thermal/humid loads.

1. Introduction

The characteristic of wave propagation in orthotropic laminated piezoelectric cylindrical shells in hydrothermal environment can be used to predict the size of damage in a structure or used in the ultrasonic inspection techniques and structural health monitoring. Wave propagation in cylindrical shells was presented based on a membrane shell model was put forth by Love (1944), in which the transverse forces, bending and twisting moments are negligible. However, the membrane shell model is only suitable for thin shell structures in which only the normal and shear forces acting in the mid-surface of shell are considered. For shells of moderate thickness, Mirsky and Herrmann (1957) presented the shear effects in both axial and circumferential directions and the rotary-inertia effects in the study of axially symmetric wave propagation in a cylindrical shell. Lin and Morgan (1956) developed the equations for axially symmetric motions including both shear and rotary-inertia effects for non-axially symmetric motion of shell structures. Cooper and Naghdi (1957) presented a theory including shear and rotary inertia effects for non-axially symmetric motion of

† Doctor, Corresponding author, E-mail: dongke@sjtu.edu.cn
‡ Professor, E-mail: xwang@sjtu.edu.cn

shell structures. Mirsky (1964) gave an approximate theory for vibration of orthotropic thick cylindrical shell in which the effect of transverse normal stress was retained, the result showed frequencies for fourth and fifth mode at infinite wavelength are very close and nearly equal for thin shell, but the result can be different by approximately 20% for thick shell. Another study of wave propagation in cylindrical shells using different shell theory by Greenspon (1960) showed that Cooper-Naghdi theory considering only the transverse shear and rotary inertia can be applied in all shells and the max error is less than 20%.

Recently, the use of piezoelectric materials in intelligent structures attracted extensive attentions. Due to the intrinsic, direct and converse piezoelectric effects, piezoelectric materials can be effectively used as sensors or actuators for the active shape or vibration control of structures. Liew (1997) and Lim (1995, 1996, 1997, 1998, 2006) studied the vibration of laminated structures with the higher order theory. Wave propagation and vibration in pure piezoelectric structures have been investigated by Mindlin (1952). The constitutive relationship of orthotropic piezoelectric materials is investigated by Ping (2002). Wang (2001, 2002, 2003) gave some original works on wave propagation in piezoelectric coupled cylinder considering transverse shear and rotary inertia. Wang (2003) presented an analytical solution for the axisymmetric deformations of a finitely long laminated cylindrical shell under pressuring loading and a uniform temperature change. However, the investigation on the effect of thermal load on wave propagation in laminated piezoelectric cylindrical shells is a few.

The effect of transverse shear, rotary inertia and thermal or humid load on wave propagation in orthotropic host cylindrical shells coupled with piezoelectric actuator layer and piezoelectric sensor layer is studied as an example in this paper. A dynamic model of laminated piezoelectric cylindrical shell is derived based on Cooper-Naghdi shell theory considering the effects of transverse shear and rotary inertia in section 2. Then, the wave characteristics curves are obtained by solving an eigenvalue problem in section 3. Besides discussing the characteristics curves in different wave modes, we also analyze the effects of the layer numbers and the thickness of piezoelectric layers and thermal/humid loads on the wave characteristics curves in section 4. Results carried out are validated by the classical solution of an elastic shell no considering the effects of transverse shear and rotary inertia, and this solution method may be used as a useful reference to investigate wave propagation in laminated piezoelectric cylindrical shells with various laminated material, the layer numbers and the thickness of piezoelectric layer not only in thermal environment but also in humid environment.

2. Governing equation

The structure studied in this article is considered as an infinitely long laminated piezoelectric cylindrical shell composed of composite host layer (1), piezoelectric actuator layer (2) and piezoelectric sensor layer (3), which is shown in Fig. 1. The coordinate system (x, θ, z) is taken, where the x axis expresses the length direction of the shell, θ expresses circumferential coordinate and z expresses radial coordinate. $z = 0$ is set on the middle surface of the laminated shell and R is the radius of the middle surface. The displacement considering the shear and rotary inertias can be written as Cooper (1957)

$$U_x(x, \theta, z, t) = u_x(x, \theta, t) + z\beta_x(x, \theta, t), \quad U_\theta(x, \theta, z, t) = u_\theta(x, \theta, t) + z\beta_\theta(x, \theta, t)$$
$$U_z(x, \theta, z, t) = w(x, \theta, t) \tag{1}$$

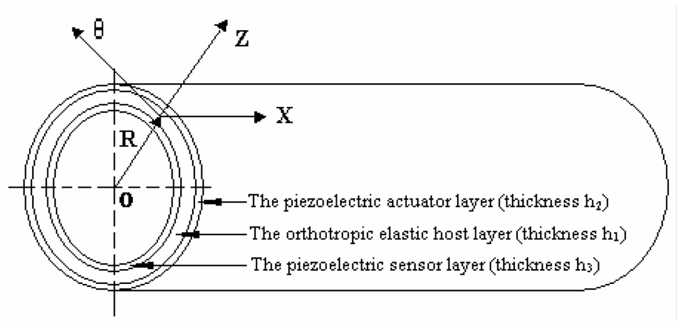

Fig. 1 Laminated piezoelectric cylindrical shell

where u_x, u_θ, w are the displacement component of a point on the midplane of the shell along the coordinate axis (x, θ, z). β_x and β_θ represent the rotations of a transverse normal at $z = 0$ about the x and θ axes, respectively, which bring in the axial and circumferential shear effects. The normal strains ε_{xx} and $\varepsilon_{\theta\theta}$, the in-plane shear strains $\gamma_{x\theta}$, and the out-plane shear strain γ_{xz} and $\gamma_{\theta z}$ can be expressed as

$$\varepsilon_{xx} = \frac{\partial u_x}{\partial x} + z\frac{\partial \beta_x}{\partial x}, \quad \varepsilon_{\theta\theta} = \frac{1}{R}\left(w + \frac{\partial u_\theta}{\partial \theta}\right) + \frac{z}{R}\frac{\partial \beta_\theta}{\partial \theta}, \quad \gamma_{x\theta} = \frac{\partial u_\theta}{\partial x} + \frac{\partial u_x}{R\partial \theta} + z\left(\frac{\partial \beta_\theta}{\partial x} + \frac{\partial \beta_x}{R\partial \theta}\right)$$

$$\gamma_{xz} = \frac{\partial w}{\partial x} + \beta_x, \quad \gamma_{\theta z} = \frac{\partial w}{R\partial \theta} - \left(\frac{u_\theta}{R} - \beta_\theta\right) \tag{2}$$

The constitutive relationship of orthotropic piezoelectric cylindrical shell can be written as

$$\{\sigma^i\} = [c^i]\cdot\{\varepsilon\} - [e^i]\cdot\{E\} - [\lambda]\cdot\Theta \tag{3}$$

where the superscripts $i = 1$, 2 and 3 represent the orthotropic composite host layer ($e^1_{31p} = e^1_{33p} = e^1_{15p} = 0$), piezoelectric actuator layer and piezoelectric sensor layer respectively; For plane stress problem, the effective elastic constants are $c^i_{13p} = c^i_{13} - \frac{c^i_{12}c^i_{13}}{c^i_{11}}$, $c^i_{11p} = c^i_{11} - \frac{c^i_{12}c^i_{12}}{c^i_{11}}$, $c^i_{33p} = c^i_{33} - \frac{c^i_{13}c^i_{13}}{c^i_{11}}$ and $c^i_{jjp} = c^i_{jj} (jj = 44, 55, 66)$ respectively; $e^i_{31p} = e^i_{31} - \frac{c^i_{12}}{c^i_{11}}e^i_{31}$, $e^i_{15p} = e^i_{15}$, $e^i_{33p} = e^i_{33} - \frac{c^i_{13}}{c^{ji}_{11}}e^i_{31}$, are the effective piezoelectric constants of piezoelectric layers; E_x and E_θ express the electric fields along the axial and circumferential directions; Θ expresses temperature changes or humidity; $\lambda^i_1 = c^i_{11p}\alpha^i_\theta + c^i_{13p}\alpha^i_x$ and $\lambda^i_2 = c^i_{13p}\alpha^i_\theta + c^i_{33p}\alpha^i_x$ express thermal elastic module and α^i_x and α^i_θ are, respectively, the coefficient of thermal expansions along the axial and circumferential directions of the ith layer. In humid environment, $\lambda^i_1 = c^i_{11p}\eta^i_\theta + c^i_{13p}\eta^i_x$ and $\lambda^i_2 = c^i_{13p}\eta^i_\theta + c^i_{33p}\eta^i_x$ express humid elastic module and η^i_x and η^i_θ are, respectively, the coefficient of humid expansions along the axial and circumferential directions of the ith layer. The shear stresses $\tau^i_{xz} = kc^i_{55p}$ and $\tau^i_{\theta z} = kc^i_{66p}$, where k expresses a shear coefficient taken as 0.8333 (Mirsky 1964). Since the thickness of piezoelectric is much thinner than that of the host, the effect of piezoelectric layers on the shear coefficient can be ignored (Wang 2003).

The relationship between the electric fields and electric potential φ are defined by

$$E_x = -\frac{\partial\varphi}{\partial x}, \quad E_\theta = -\frac{\partial\varphi}{R\partial\theta} \tag{4}$$

Substituting Eq. (2) into Eq. (3) and integrating the stresses across the thickness of the shell, give the membrane forces as Wang (2003)

$$N_x = A_1\frac{\partial u_x}{\partial x} + \frac{A_2}{R}\left(w + \frac{\partial u_\theta}{\partial\theta}\right) + A_3\frac{\partial\beta_x}{\partial x} + \frac{A_4}{R}\frac{\partial\beta_\theta}{\partial\theta} + A_5\frac{\partial\varphi}{\partial x} + A_6\Theta$$

$$N_\theta = \frac{B_1}{R}\left(w + \frac{\partial u_\theta}{\partial\theta}\right) + B_2\frac{\partial u_x}{\partial x} + \frac{B_3}{R}\frac{\partial\beta_\theta}{\partial\theta} + B_4\frac{\partial\beta_x}{\partial x} + B_5\frac{\partial\varphi}{\partial x} + B_6\Theta$$

$$N_{\theta x} = N_{x\theta} = C_1\left(\frac{\partial u_\theta}{\partial x} + \frac{\partial u_x}{R\partial\theta}\right) + \frac{C_2}{R}\frac{\partial\beta_x}{\partial\theta} + C_2\frac{\partial\beta_\theta}{\partial x} + C_3\frac{\partial\varphi}{R\partial\theta}$$

$$M_x = D_1\frac{\partial\beta_x}{\partial x} + \frac{D_2}{R}\frac{\partial\beta_\theta}{\partial\theta} + D_3\frac{\partial u_x}{\partial x} + \frac{D_4}{R}\left(w + \frac{\partial u_\theta}{\partial\theta}\right) + D_5\frac{\partial\varphi}{\partial x} + D_6\Theta$$

$$M_\theta = \frac{E_1}{R}\frac{\partial\beta_\theta}{\partial\theta} + E_2\frac{\partial\beta_x}{\partial x} + \frac{E_3}{R}\left(w + \frac{\partial u_\theta}{\partial\theta}\right) + E_4\frac{\partial u_x}{\partial x} + E_5\frac{\partial\varphi}{\partial x} + E_6\Theta$$

$$M_{x\theta} = F_1\frac{\partial\beta_\theta}{\partial x} + \frac{F_1}{R}\frac{\partial\beta_x}{\partial\theta} + F_2\left(\frac{\partial u_\theta}{\partial x} + \frac{\partial u_x}{R\partial\theta}\right) + F_3\frac{\partial\varphi}{R\partial\theta}$$

$$Q_x = k(c^1_{44p}h_1 + c^2_{44p}h_2 + c^3_{44p}h_3)\left(\frac{\partial w}{\partial x} + \beta_x\right)$$

$$Q_\theta = k(c^1_{44p}h_1 + c^2_{44p}h_2 + c^3_{44p}h_3)\left(\frac{\partial w}{R\partial\theta} + \beta_\theta - \frac{u_\theta}{R}\right) \tag{5-12}$$

where N_x, N_θ and $N_{\theta x}$ are the membrane forces, M_x, M_θ and $M_{x\theta}$ are the internal moment and Q_x and Q_θ are the normal shear forces, and the expressions of A_i, B_i, C_i, D_i, E_i $(i = 1,\ldots, 6)$ and F_i $(i = 1,\ldots, 3)$ are shown in appendix A.

By considering the effects of piezoelectric layers, the dynamic equations of laminated piezoelectric cylindrical shells under thermal or humid load are written as Reissner (1941)

$$\frac{\partial N_x}{\partial x} + \frac{\partial N_{\theta x}}{R\partial\theta} = (\rho_1 h_1 + \rho_2 h_2 + \rho_3 h_3)\frac{\partial^2 u_x}{R\partial t^2} + \left[\frac{\rho_1 h_1^3}{12} + \frac{\rho_2}{3}\left(h_2^3 + \frac{3}{2}h_1 h_2^2 + \frac{3}{4}h_1^2 h_2\right)\right.$$
$$\left.+ \frac{\rho_3}{3}\left(h_3^3 + \frac{3}{2}h_1 h_3^2 + \frac{3}{4}h_1^2 h_3\right)\right]\frac{\partial^2\beta_x}{R\partial t^2}$$

$$\frac{\partial N_\theta}{R\partial_\theta} + \frac{\partial N_{x\theta}}{\partial x} + \frac{Q_\theta}{R} = (\rho_1 h_1 + \rho_2 h_2 + \rho_3 h_3)\frac{\partial^2 u_\theta}{R\partial t^2} + \left[\frac{\rho_1 h_1^3}{12} + \frac{\rho_2}{3}\left(h_2^3 + \frac{3}{2}h_1 h_2^2 + \frac{3}{4}h_1^2 h_2\right)\right.$$
$$\left.+ \frac{\rho_3}{3}\left(h_3^3 + \frac{3}{2}h_1 h_3^2 + \frac{3}{4}h_1^2 h_3\right)\right]\frac{\partial^2\beta_\theta}{R\partial t^2}$$

$$\frac{\partial Q_x}{\partial x}+\frac{\partial Q_\theta}{R\partial\theta}-\frac{N_\theta}{R} = (\rho_1 h_1+\rho_2 h_2+\rho_3 h_3)\frac{\partial^2 w}{\partial t^2}$$

$$\frac{\partial M_x}{\partial x}+\frac{\partial M_{x\theta}}{R\partial\theta}-Q_x=\left[\frac{\rho_1 h_1^3}{12}+\frac{\rho_2}{3}\left(h_2^3+\frac{3}{2}h_1h_2^2+\frac{3}{4}h_1^2h_2\right)+\frac{\rho_3}{3}\left(h_3^3+\frac{3}{2}h_1h_3^2+\frac{3}{4}h_1^2h_3\right)\right]\times\left(\frac{\partial^2\beta_x}{\partial t^2}+\frac{\partial^2 u_x}{R\partial t^2}\right)$$

$$\frac{\partial M_{x\theta}}{\partial x}+\frac{\partial M_\theta}{R\partial\theta}-Q_\theta=\left[\frac{\rho_1 h_1^3}{12}+\frac{\rho_2}{3}\left(h_2^3+\frac{3}{2}h_1h_2^2+\frac{3}{4}h_1^2h_2\right)+\frac{\rho_3}{3}\left(h_3^3+\frac{3}{2}h_1h_3^2+\frac{3}{4}h_1^2h_3\right)\right]\times\left(\frac{\partial^2\beta_\theta}{\partial t^2}+\frac{\partial^2 u_\theta}{R\partial t^2}\right)$$

(13-17)

where ρ_1, ρ_2 and ρ_3 express the mass densities of the elasticity host shell, the piezoelectric actuator layer and the piezoelectric sensor layer.

3. Dispersion characteristics

Substituting Eqs. (5-12) into Eqs. (13-17) yields the following five equations of laminated piezoelectric cylinder shells in terms of u_x, u_θ, w, β_x and β_θ as follows

$$A_1\frac{\partial^2 u_x}{\partial x^2}+\frac{A_2}{R}\left(\frac{\partial w}{\partial x}+\frac{\partial^2 u_\theta}{\partial x\partial\theta}\right)+A_3\frac{\partial^2\beta_x}{\partial x^2}+\frac{A_4}{R}\frac{\partial^2\beta_\theta}{\partial x\partial\theta}+A_5\frac{\partial^2\varphi}{\partial x^2}+\frac{C_1}{R}\left(\frac{\partial^2 u_\theta}{\partial\theta\partial x}+\frac{\partial^2 u_x}{R\partial\theta^2}\right)$$

$$+C_2\frac{\partial^2\beta_x}{R^2\partial\theta^2}+\frac{C_2}{R}\frac{\partial^2\beta_\theta}{\partial x\partial\theta}+C_3\frac{\partial^2\varphi}{R^2\partial\theta^2}+A_6\frac{\partial\Theta}{\partial x} = (\rho_1h_1+\rho_2h_2+\rho_3h_3)\frac{\partial^2 u_x}{R\partial t^2}$$

$$+\left[\frac{\rho_1 h_1^3}{12}+\frac{\rho_2}{3}\left(h_2^3+\frac{3}{2}h_1h_2^2+\frac{3}{4}h_1^2h_2\right)+\frac{\rho_3}{3}\left(h_3^3+\frac{3}{2}h_1h_3^2+\frac{3}{4}h_1^2h_3\right)\right]\frac{\partial^2\beta_x}{R\partial t^2},$$

$$\frac{B_1}{R^2}\left(\frac{\partial w}{\partial\theta}+\frac{\partial^2 u_\theta}{\partial\theta^2}\right)+\frac{B_2}{R}\frac{\partial^2 u_x}{\partial x\partial\theta}+\frac{B_3}{R^2}\frac{\partial^2\beta_\theta}{\partial\theta^2}+\frac{B_4}{R}\frac{\partial^2\beta_x}{\partial x\partial\theta}+\frac{B_5}{R}\frac{\partial^2\varphi}{\partial x\partial\theta}+C_1\left(\frac{\partial^2 u_\theta}{\partial x^2}+\frac{\partial^2 u_x}{R\partial x\partial\theta}\right)$$

$$+C_2\frac{\partial^2\beta_x}{\partial\theta^2}+C_2\frac{\partial^2\beta_\theta}{\partial x^2}+C_3\frac{\partial^2\varphi}{R\partial x\partial\theta}+\frac{k}{R}(c_{44p}^1h_1+c_{44p}^2h_1+c_{44p}^3h_2)\left(\frac{\partial w}{R\partial\theta}+\beta_\theta-\frac{u_\theta}{R}\right)+\frac{B_6\partial\Theta}{R\partial\theta}$$

$$= (\rho_1h_1+\rho_2h_2+\rho_3h_3)\frac{\partial^2 u_\theta}{R\partial t^2}+\left[\frac{\rho_1 h_1^3}{12}+\frac{\rho_2}{3}\left(h_2^3+\frac{3}{2}h_1h_2^2+\frac{3}{4}h_1^2h_2\right)\right.$$

$$\left.+\frac{\rho_3}{3}\left(h_3^3+\frac{3}{2}h_1h_3^2+\frac{3}{4}h_1^2h_3\right)\right]\frac{\partial^2\beta_\theta}{R\partial t^2},$$

$$k\left(\frac{Eh}{2(1+\mu)}+c_{44p}^2h_2+c_{44p}^3h_3\right)\left(\frac{\partial^2 w}{\partial x^2}+\frac{\partial\beta_x}{\partial x}+\frac{\partial^2 w}{R^2\partial\theta^2}+\frac{\partial\beta_\theta}{R\partial\theta}-\frac{\partial u_\theta}{R^2\partial\theta}\right)$$

$$-\frac{B_1}{R^2}\left(w+\frac{\partial u_\theta}{\partial\theta}\right)-\frac{B_2}{R}\frac{\partial u_x}{\partial x}-\frac{B_3}{R^2}\frac{\partial\beta_\theta}{\partial\theta}-\frac{B_4}{R}\frac{\partial\beta_x}{\partial x}-\frac{B_5}{R}\frac{\partial\varphi}{\partial x}-\frac{B_6}{R}T = (\rho_1h_1+\rho_2h_2+\rho_3h_3)\frac{\partial^2 w}{\partial t^2},$$

$$D_1\frac{\partial^2\beta_x}{\partial x^2}+\frac{D_2}{R}\frac{\partial^2\beta_\theta}{\partial x\partial\theta}+D_3\frac{\partial^2 u_x}{\partial x^2}+\frac{D_4}{R}\left(\frac{\partial w}{\partial x}+\frac{\partial^2 u_\theta}{\partial x\partial\theta}\right)+D_5\frac{\partial^2\varphi}{\partial x^2}+F_1\frac{\partial^2\beta_\theta}{R\partial x\partial\theta}+\frac{F_1}{R^2}\frac{\partial^2\beta_x}{\partial\theta^2}$$
$$+F_2\left(\frac{\partial^2 u_\theta}{R\partial x\partial\theta}+\frac{\partial^2 u_x}{R^2\partial\theta^2}\right)+F_3\frac{\partial^2\varphi}{R^2\partial\theta^2}-k(c^1_{44p}h_1+c^2_{44p}h_2+c^3_{44p}h_3)\left(\frac{\partial w}{\partial x}+\beta_x\right)+D_6\frac{\partial\Theta}{\partial x}$$
$$=\left[\frac{\rho_1 h_1^3}{12}+\frac{\rho_2}{3}\left(h_2^3+\frac{3}{2}h_1h_2^2+\frac{3}{4}h_1^2h_2\right)+\frac{\rho_3}{3}\left(h_3^3+\frac{3}{2}h_1h_3^2+\frac{3}{4}h_1^2h_3\right)\right]\left(\frac{\partial^2\beta_x}{\partial t^2}+\frac{\partial^2 u_x}{R\partial t^2}\right),$$

$$F_1\frac{\partial^2\beta_\theta}{\partial x^2}+\frac{F_1}{R}\frac{\partial^2\beta_x}{\partial x\partial\theta}+F_2\left(\frac{\partial^2 u_\theta}{\partial x^2}+\frac{\partial^2 u_x}{R\partial x\partial\theta}\right)+F_3\frac{\partial^2\varphi}{R\partial x\partial\theta}+\frac{E_1}{R^2}\frac{\partial^2\beta_\theta}{\partial\theta^2}+E_2\frac{\partial^2\beta_x}{R\partial x\partial\theta}+\frac{E_3}{R^2}\left(\frac{\partial w}{\partial\theta}+\frac{\partial^2 u_\theta}{\partial\theta^2}\right)$$
$$+E_4\frac{\partial^2 u_x}{R\partial x\partial\theta}+E_5\frac{\partial^2\varphi}{\partial x\partial\theta}-k(c^1_{44p}h_1+c^2_{44p}h_1+c^3_{44p}h_2)\left(\frac{\partial w}{R\partial\theta}+\beta_\theta-\frac{u_\theta}{R}\right)+E_6\frac{\partial\Theta}{R\partial\theta}$$
$$=\left[\frac{\rho_1 h_1^3}{12}+\frac{\rho_2}{3}\left(h_2^3+\frac{3}{2}h_1h_2^2+\frac{3}{4}h_1^2h_2\right)+\frac{\rho_3}{3}\left(h_3^3+\frac{3}{2}h_1h_3^2+\frac{3}{4}h_1^2h_3\right)\right]\left(\frac{\partial^2\beta_\theta}{\partial t^2}+\frac{\partial^2 u_\theta}{R\partial t^2}\right)\quad(18\text{-}22)$$

The electric displacements in the piezoelectric actuator layer and sensor layer are expressed as

$$D_x^2=-\Xi^2_{33p}\frac{\partial\varphi}{\partial x}+e^2_{33p}\varepsilon_x+e^2_{31p}\varepsilon_\theta+p_3^2\Theta,\quad D_\theta^2=-\Xi^2_{11p}\frac{\partial\varphi}{R\partial\theta}+e^2_{15p}\gamma_{x\theta},\quad D_z^2=e^2_{15p}\gamma_{xz}\quad(23)$$

$$D_x^3=-\Xi^3_{33p}\frac{\partial\varphi}{\partial x}+e^3_{33p}\varepsilon_x+e^3_{31p}\varepsilon_\theta+p_3^3\Theta,\quad D_\theta^3=-\Xi^3_{11p}\frac{\partial\varphi}{R\partial\theta}+e^3_{15p}\gamma_{x\theta},\quad D_z^3=e^3_{15p}\gamma_{xz}\quad(24)$$

where $\Xi^i_{33p}=\Xi^i_{33}+\dfrac{e^i_{31}e^i_{31}}{c^i_{11}}$, $\Xi^i_{11p}=\Xi^i_{11}+\dfrac{e^i_{15}e^i_{15}}{c^i_{55}}$ ($i=2,3$), are the effective dielectric coefficients in the piezoelectric layers for a plane stress problem. The superscripts 2 and 3 represent, respectively, the piezoelectric actuator layer and the piezoelectric sensor layer. p_3^2 and p_3^3 represent the pyroelectric coefficients in piezoelectric actuator layer and the piezoelectric sensor layer respectively.

Because the piezoelectric actuator layer and the piezoelectric sensor should, respectively, meet Maxwell equation $\int\nabla D dz=0$, we have

$$-\Xi^2_{33p}\frac{\partial^2\varphi}{\partial x^2}-\Xi^2_{11p}\frac{\partial^2\varphi}{R^2\partial\theta^2}+e^2_{33p}\frac{\partial^2 u_x}{\partial x^2}+\frac{e^2_{33p}}{2}(h_1+h_2)\frac{\partial^2\beta_x}{\partial x^2}+\frac{e^2_{31p}}{R}\left(\frac{\partial w}{\partial x}+\frac{\partial^2 u_\theta}{\partial x\partial\theta}\right)$$
$$+\frac{e^2_{31p}}{2R}(h_1+h_2)\frac{\partial^2\beta_\theta}{\partial\theta\partial x}+e^2_{15p}\left(\frac{\partial^2 u_\theta}{R\partial x\partial\theta}+\frac{\partial^2 u_x}{R^2\partial\theta^2}\right)+\frac{e^2_{15p}}{2}(h_1+h_2)\left(\frac{\partial^2\beta_\theta}{R\partial x\partial\theta}+\frac{\partial^2\beta_x}{R^2\partial\theta^2}\right)+p_3^2\frac{\partial\Theta}{\partial x}=0$$

$$-\Xi^3_{33p}\frac{\partial^2\varphi}{\partial x^2}-\Xi^3_{11p}\frac{\partial^2\varphi}{R^2\partial\theta^2}+e^3_{33p}\frac{\partial^2 u_x}{\partial x^2}-\frac{e^3_{33p}}{2}(h_1+h_3)\frac{\partial^2\beta_x}{\partial x^2}+\frac{e^3_{31p}}{R}\left(\frac{\partial w}{\partial x}+\frac{\partial^2 u_\theta}{\partial x\partial\theta}\right)$$

$$-\frac{e_{31p}^{3}}{2R}(h_1+h_3)\frac{\partial^2\beta_\theta}{\partial\theta\partial x}+e_{15p}^{3}\left(\frac{\partial^2 u_\theta}{R\partial x\partial\theta}+\frac{\partial^2 u_x}{R^2\partial\theta^2}\right)-\frac{e_{15p}^{3}}{2}(h_1+h_3)\left(\frac{\partial^2\beta_\theta}{R\partial x\partial\theta}+\frac{\partial^2\beta_x}{R^2\partial\theta^2}\right)+p_3^3\frac{\partial\Theta}{\partial x}=0 \tag{25-26}$$

Wave propagation in thermal environment is studied by considering the following solutions:

$$u_x(x,\theta,t)=Ue^{i\xi(x-ct)}\cos n\theta,\quad u_\theta(x,\theta,t)=Ve^{i\xi(x-ct)}\sin n\theta,\quad w(x,\theta,t)=We^{i\xi(x-ct)}\cos n\theta$$

$$\beta_x(x,\theta,t)=B_x e^{i\xi(x-ct)}\cos n\theta,\quad \beta_\theta(x,\theta,t)=B_\theta e^{i\xi(x-ct)}\sin n\theta,\quad \varphi(x,\theta,t)=\phi e^{i\xi(x-ct)}\cos n\theta$$

$$\Theta(x,\theta,t)=\Gamma e^{i\xi(x-ct)}\cos n\theta \tag{27-33}$$

where ξ and c are the wave number and wave phase velocity respectively, and $\omega=\xi c$ is the corresponding frequency.

Substituting Eqs. (27-33) into Eqs. (18-22) and Eqs. (25-26) yields a set of homogeneous equations in terms of $U, V, W, \beta_x, \beta_\theta, \phi, \Gamma$ as:

$$\begin{bmatrix} a_{11} & a_{12} & a_{13} & a_{14} & a_{15} & a_{16} & a_{17} \\ a_{21} & a_{22} & a_{23} & a_{24} & a_{25} & a_{26} & a_{27} \\ a_{31} & a_{32} & a_{33} & a_{34} & a_{35} & a_{36} & a_{37} \\ a_{41} & a_{42} & a_{43} & a_{44} & a_{45} & a_{46} & a_{47} \\ a_{51} & a_{52} & a_{53} & a_{54} & a_{55} & a_{56} & a_{57} \\ a_{61} & a_{62} & a_{63} & a_{64} & a_{65} & a_{66} & a_{67} \\ a_{71} & a_{72} & a_{73} & a_{74} & a_{75} & a_{76} & a_{77} \end{bmatrix}\begin{Bmatrix} U \\ V \\ W \\ \beta_x \\ \beta_\theta \\ \phi \\ \Gamma \end{Bmatrix}=\{0\} \tag{34}$$

where the expressions of $a_{ij}(i=1,\ldots,7;\, j=1,\ldots,7)$ are shown in appendix B. The relationship between the wave number ξ and wave phase velocity c is determined by searching the condition for non-trivial solution of $U, V, W, \beta_x, \beta_\theta, \phi, \Gamma$.

According to any specific wave number ξ, the wave phase velocity c can be determined from the non-trivial solution of Eq. (35). Using this method, wave characteristics curves in thermal or humid environment for different modes are obtained.

4. Results and discussions

In numerical examples, the outer piezoelectric actuator layer adopts PZT-4 material, and the thickness is h_2; The inner piezoelectric sensor layer adopts PVDF material, and the thickness is h_3. The all material properties (Kadoli 2004) are listed in appendix C.

To easily investigate the effect of piezoelectric layers, the non-dimensional wave number of wave characteristics curves is taken as $\xi h/2\pi$ and the non-dimensional velocity is taken as c/c_t (Wang 2003) where

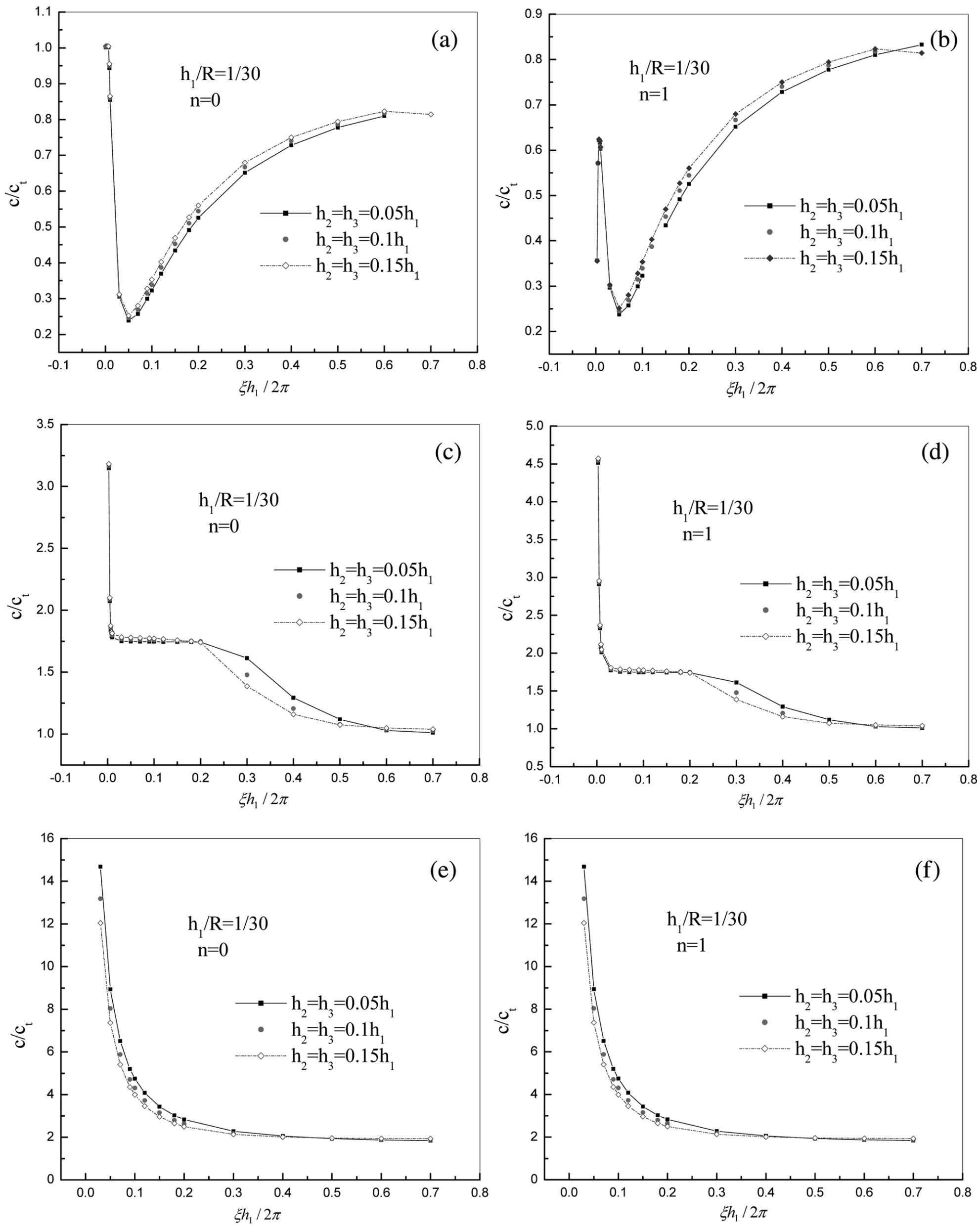

Fig. 2 The effect of thickness on wave characteristics curves for the first mode at (a) $n = 0$ and (b) $n = 1$, for the second mode at (c) $n = 0$ and (d) $n = 1$ and for the fifth mode at (e) $n = 0$ and (f) $n = 1$

$$c_t = \left[\frac{c_{44p}^1 h_1 + c_{44p}^2 h_2 + c_{44p}^3 h_3 - c_{44p}^2 \dfrac{(h_1 h_2 + h_2^2)}{R} + c_{44p}^3 \times \dfrac{(h_1 h_3 + h_2^2)}{R}}{\rho_1 h_1 + \rho_2 h_2 + \rho_3 h_3}\right]^{1/2}$$

The effect of piezoelectric layer's thickness on the wave propagation, characteristics curves of the

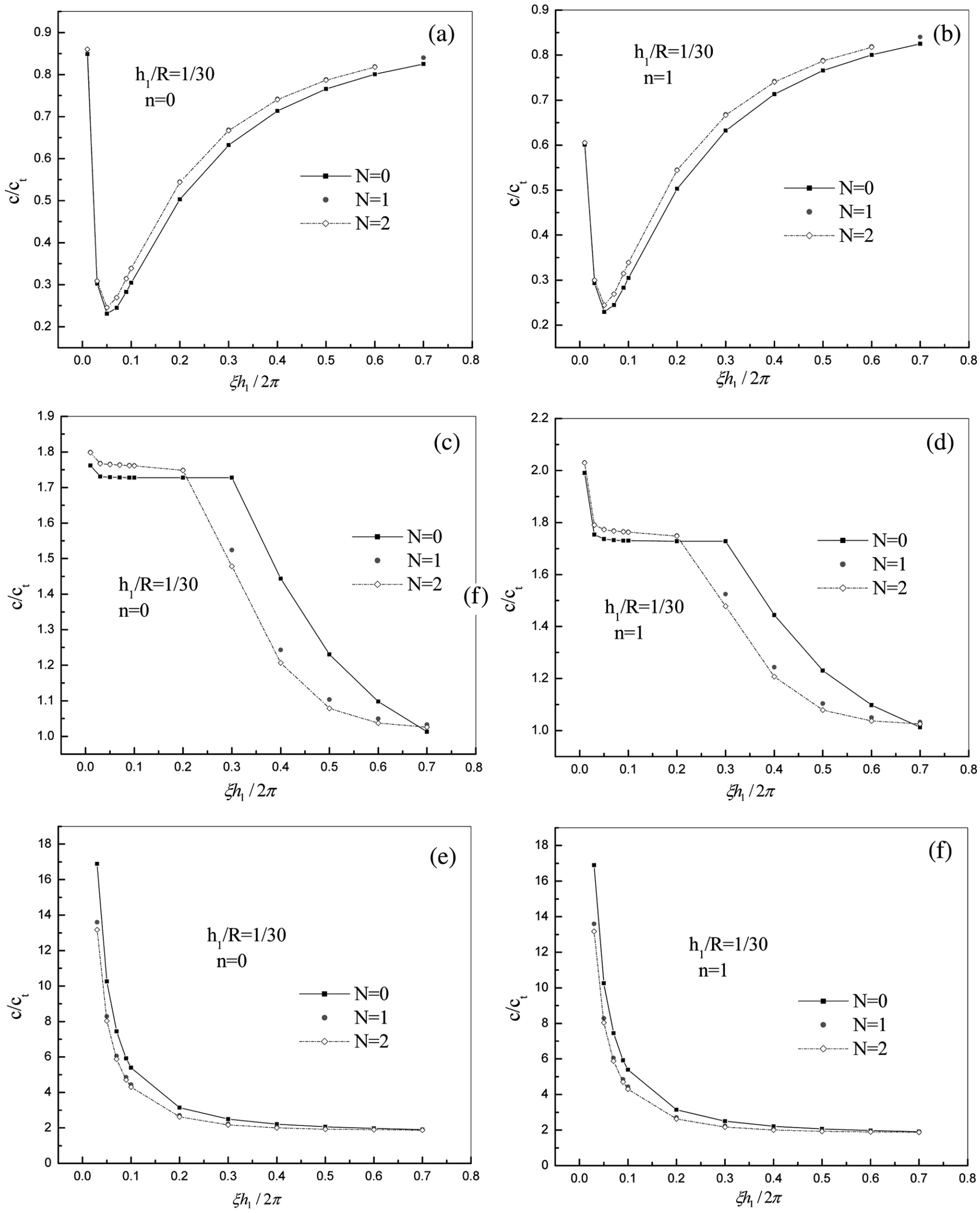

Fig. 3 The effect of piezoelectric layer numbers on wave characteristics curves for the first mode at (a) $n = 0$ and (b) $n = 1$, for the third mode at (c) $n = 0$ and (d) $n = 1$ and for the fifth mode at (e) $n = 0$ and (f) $n = 1$

first, second and fifth modes at $h_2 = h_3 = 0.05h_1, 0.1h_1, 0.15h_1$, when $n = 0$ and $n = 1$ are plotted in Fig. 2. The result shows that the phase velocity drastic increases as the wave mode increases; besides, the lower the ratio of the thickness of elastic host layer to the thickness of piezoelectric layer is, the higher the velocity is. The characteristics curves of the first mode when $n = 0$ and $n = 1$ are shown in Figs. 2(a) and (b). It is evident that the phase velocity decreases dramatically within a very small range of wave number at first, and then it varies smoothly with higher wave number. Similar phenomena for the second mode when $n = 0$ and $n = 1$ is also shown in Figs. 2(c) and (d). It is seen that the phase velocity decreases as wave numbers increase, and the difference of the velocity is very evidence in larger wave number. The characteristics curves of the fifth mode for $n = 0$ and $n = 1$ are shown in Figs. 2(e) and (f). It is seen that wave velocity differs form each other at lower wave number, and wave velocity convergence to a fixed value at higher wave number, which is independent on the thickness of piezoelectric layers.

The effect of piezoelectric layer numbers on wave propagation is discussed in this segment. The characteristics curve of the first, third and fifth modes at $h_2 = h_3 = 0.1h_1$ when $n = 0$ and $n = 1$ with 1, 2 and 3 layers are plotted in Fig. 3. The result shows that the characteristics curves of different piezoelectric laminated shells appear in the same change tendency, but the effect of different piezoelectric layers on wave velocity is very evidence. The characteristics curves of the first mode when $n = 0$ and $n = 1$ are shown in Figs. 3(a) and (b). It is seen that the phase velocity increases as the layer numbers of piezoelectric layer increase, on the other hand, the velocity for the third and fifth modes decreases as the piezoelectric layers increase which is, respectively, shown in Figs. 3(c), (d) and (e), (f). It is also found that the velocity in laminated cylindrical shells with more than two piezoelectric layers is very close.

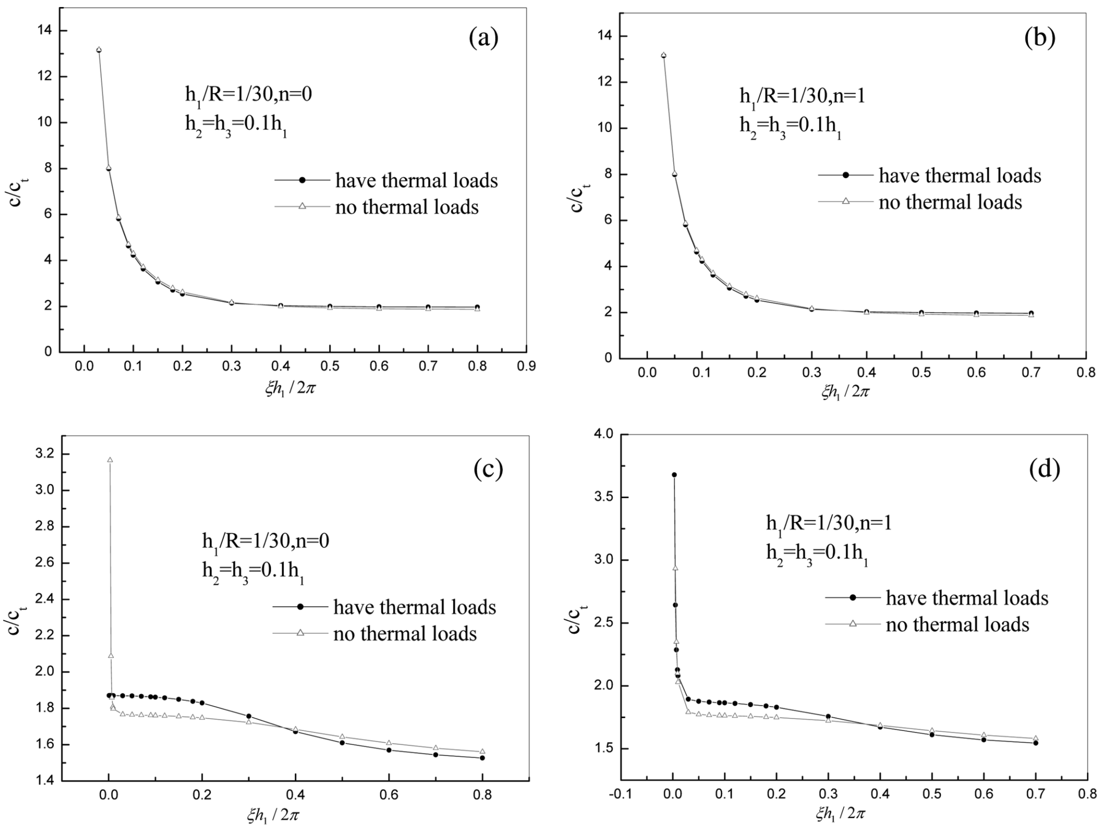

Fig. 4 The effect of thermal loads on wave characteristics curve for the first mode at (a) $n = 0$ and (b) $n = 1$, for the fifth mode at (c) $n = 0$ and (d) $n = 1$

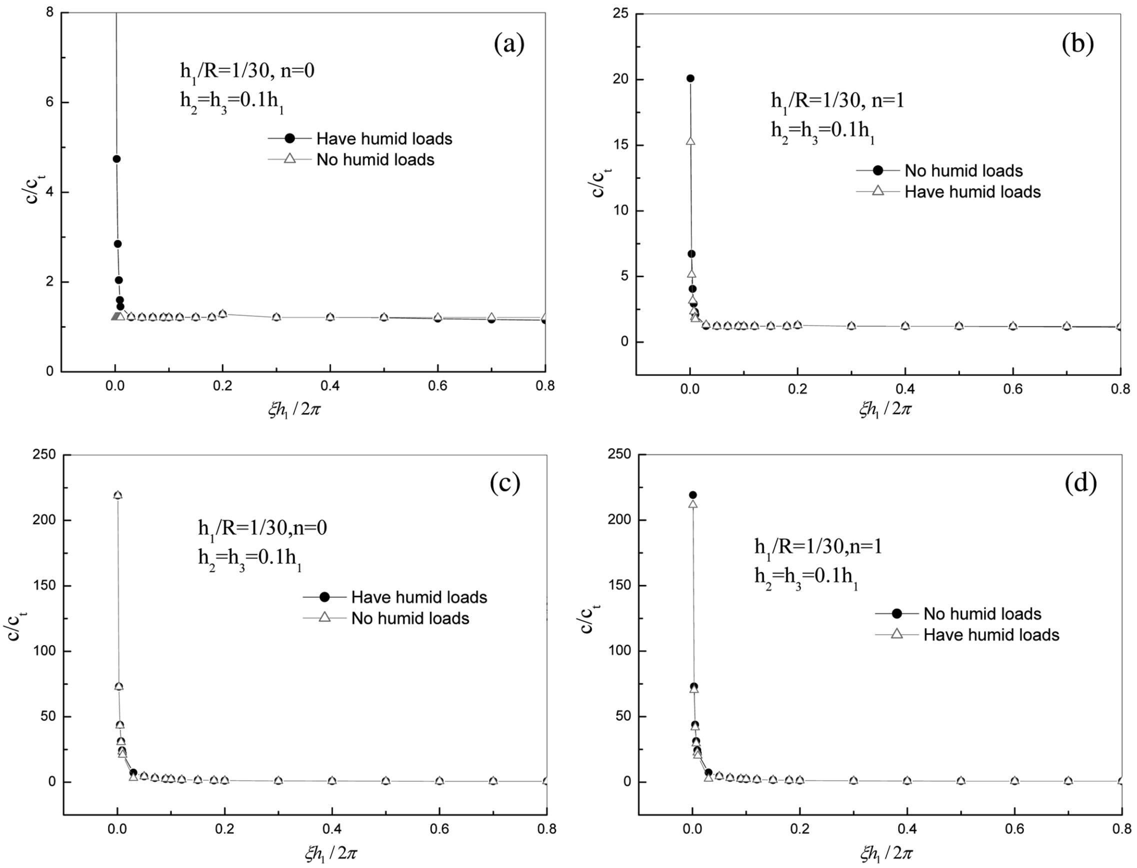

Fig. 5 The effect of humid loads on wave characteristics curve for the third mode at (a) $n = 0$ and (b) $n = 1$, for the fourth mode at (c) $n = 0$ and (d) $n = 1$

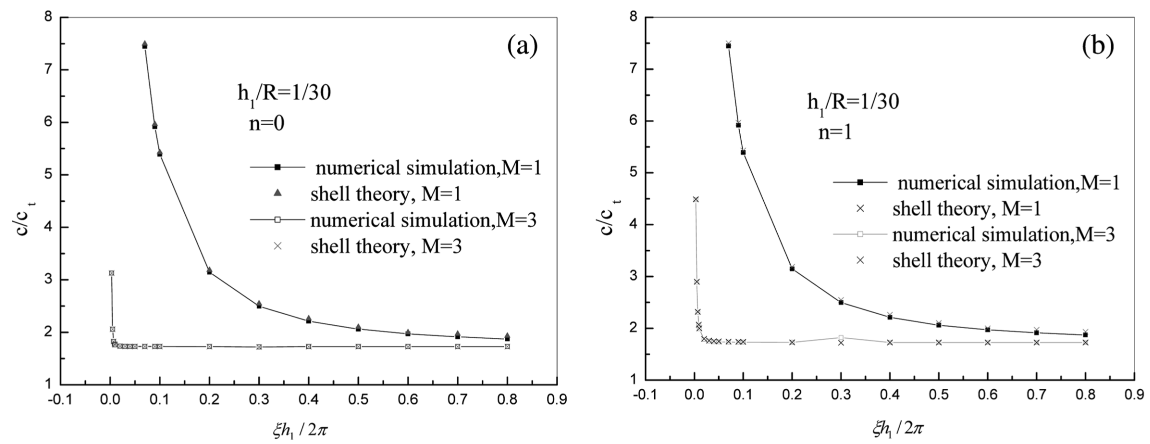

Fig. 6 A comparison of wave characteristics curves from two different methods at (a) $n = 0$ and (b) $n = 1$, where M expresses Modes

The effect of the thermal loads on the characteristics curves in the first and fifth modes at $h_2 = h_3 = 0.1h_1$ for $n = 0$ and $n = 1$ are described in Fig. 4. The result shows that the effect of thermal loads on wave propagation is drastic for only the fifth wave mode, the magnitude of phase velocity is very lower when piezoelectric laminated cylindrical shells under thermal load (which can't be obviously shown in the characteristics curve), but for the first mode at $n = 0$ and $n = 1$, the effect of thermal loads on wave velocity is very lower which is shown in Figs. 4(a), (b). For the fifth mode at $n = 0$ and $n = 1$ (Figs. 4(c) and (d)), the influence of temperature change on phase velocity is very evidence. The effect of the humid loads on the characteristics curves in the third and fourth modes are described in Fig. 5. The host layer is taken as fiber layer. The two piezoelectric layers take PZT-4 as sensors. The result shows that the effect of humid loads on wave propagation is very low.

In order to comparison with the published literature by Mirsky and Herrmann (1957), the elasticity host layer, with the thickness h_1, is taken as Aluminum. The wave characteristics curve for the two wave modes at $n = 0$ and $n = 1$ when $h_1/R = 1/30$, $h_2 = h_3 = 0$ and $\Theta = 0$ (no considering piezoelectric layer and temperature/humidity changes) obtained from two different methods are described in Fig. 6. These curves carried out in the paper are the same as those presented by Mirsky and Herrmann (1957) for pure elastic shell problem.

5. Conclusions

The main contribution in the paper is to describe the effects of transverse shear, rotary inertia and thermal/humid loads on wave propagation in orthotropic piezoelectric laminated cylindrical shells. The effects of the layers number, thickness of piezoelectric layers and thermal/humid loads on the wave propagation and the wave characteristics curves are concluded by

(1) The phase velocity drastic increases as wave modes increase, besides, the velocity is higher when the thickness ratio of elastic host layer to the thickness of piezoelectric layer is lower;

(2) The velocity in the first mode increases as the layer numbers of piezoelectric layer increase, but the velocity in the third and fifth modes decreases as the layer numbers of piezoelectric layer increase, the velocity is very close when there are more than two piezoelectric layers coupled with cylindrical shell;

(3) The effect of thermal loading on wave propagation in an orthotropic laminated piezoelectric cylindrical shells is drastic for the fifth wave mode, but for the first mode the effect is very lower. The effect of humid loading on wave propagation is little.

The solution method in the paper may be used as a useful reference to investigate wave propagation in laminated piezoelectric coupled cylindrical shell not only in thermal environment but also in humid environment, for various laminated materials, the layers numbers and the thickness of piezoelectric layer.

References

Cooper, R.M. and Naghdi, P.M. (1957), "Propagation of non-axially symmetric waves in elastic cylindrical shells", *J. Acoust. Soc. Am.,* **29**, 1365-1372.

Greenspon, J.E. (1960), "Vibrations of a thick-walled cylindrical shell comparison of the exact theory with

approximate theories", *J. Acoust. Soc. Am.,* **32**, 571-578.
Kadoli, R.K. and Ganesan, N. (2004), "Studies on dynamic behavior of composite and isotropic cylindrical shells with PZT layers under axisymmetric temperature variation", *J. Sound Vib.,* **271**, 103-130.
Liew, K.M., Lim, C.W. and Kitipornchai, S. (1997), "Vibration of shallow shells: A review with bibliography", *Appl. Mech. Rev.*, **50**, 431-444.
Liew, C.W., Cheng, Z.Q. and Reddy, J.N. (2006), "Natural frequencies of laminated piezoelectric plates with internal electrodes", *ZAMM*, **86**, 410-420.
Lim, C.W. and Liew, K.M. (1995), "A higher order theory for vibration of shear deformable cylindrical shallow shells", *Int. J. Mech. Sci.*, **37**, 277-295.
Lim, C.W. and Liew, K.M. (1996), "Vibration of moderately thick cylindrical shallow shells", *J. Acoust. Soc. Am.*, **100**, 3665-3673.
Lim, C.W., Liew, K.M. and Kitipornchai, S. (1998), "Vibration of open cylindrical shells: A three-dimensional elasticity approach", *J. Acoust. Soc. Am.*, **104**, 1436-1443.
Love, A.E.H. (1944), *A Treatise on the Mathematical Theory of Elasticity.* Dover Publication, New York.
Lin, T.C. and Morgan, G.W. (1956), "A study axi-symmetric vibrations of cylindrical shells as affected by rotary inertia and transverse shear", *J. Appl. Mech.,* **23**, 255-261.
Mindlin, R.D. (1952), "Forced thickness-shear and flexural vibrations of piezoelectric crystal plates", *J. Appl. Phy.,* **23**, 83-88.
Mirsky, I. (1964), "Vibrations of orthotropic, thick, cylindrical shells", *J. Acoust. Soc. Am.,* **36**, 41-51.
Mirsky, I. and Herrmann, G. (1957), "Non-axially symmetric motions of cylindrical shells", *J. Acoust. Soc. Am.,* **29**, 1116-1123.
Ping, T. and Li, Y.T. (2002), "Modeling for the electro-magneto-elastic properties of piezoelectric-magnetic fiber reinforced composites", *Composites, A: Spplied Science and Manufacturing,* **33**, 631-645.
Reissner, E. (1941), "A new derivation of the equations for the deformation of elastic shells", *Am. J. Math.,* **63**, 177-184.
Wang, Q. (2001), "Wave propagation in a piezoelectric coupled cylindrical membrane shell", *Int. J. Solids Struct.*, **38**, 8207-8218.
Wang, Q. (2002), "Axi-symmetric wave propagation in a cylinder coated with a piezoelectric layer", *Int. J. Solids Struct.,* **39**, 3023-3027.
Wang, Q. (2003), "Analysis of wave propagation in piezoelectric coupled cylinder affected by transverse shear and rotary inertia", *Int. J. Solids Struct.*, **40**, 6653-6667.
Wang, X. (2003), "A finitely long circular cylindrical shell of piezoelectric/piezomagnetic composite under pressuring and temperature change", *Int. J. Eng. Sci.*, **41**, 2429-2445.

Appendix A

$$A_1 = c^1_{33p}h_1 + c^2_{33p}h_2 + c^3_{33p}h_3, \quad A_2 = c^1_{13p}h_1 + c^2_{13p}h_2 + c^3_{13p}h_3$$

$$A_3 = \frac{1}{2}c^2_{33p}(h_2^2 + h_1h_2) - \frac{1}{2}c^3_{33p}(h_3^2 + h_1h_3), \quad A_4 = \frac{1}{2}c^2_{13p}(h_2^2 + h_1h_2) - \frac{1}{2}c^3_{13p}(h_3^2 + h_1h_3)$$

$$A_5 = e^2_{33p}h_2 + e^3_{33p}h_3, \quad A_6 = -\lambda^1_2h_1 - \lambda^2_2h_2 - \lambda^3_2h_3, \quad B_1 = c^1_{11p}h_1 + c^2_{11p}h_2 + c^3_{11p}h_3, \quad B_2 = A_2$$

$$B_3 = \frac{1}{2}c^2_{11p}(h_2^2 + h_1h_2) - \frac{1}{2}c^3_{11p}(h_3^2 + h_1h_3), \quad B_4 = A_4, \quad B_5 = e^2_{31p}h_2 + e^3_{31p}h_3$$

$$B_6 = -\lambda^2_1h_1 - \lambda^2_1h_2 - \lambda^3_1h_3, \quad C_1 = c^1_{44p}h_1 + c^2_{44p}h_2 + c^3_{44p}h_3$$

$$C_2 = \frac{1}{2}c^2_{44p}(h_2^2 + h_1h_2) - \frac{1}{2}c^3_{44p}(h_3^2 + h_1h_3), \quad C_3 = e^2_{15p}h_2 + e^3_{15p}h_3$$

$$D_1 = \frac{1}{12}c_{33p}^1 h_1^3 + \frac{c_{33p}^2}{3}\left(h_2^3 + \frac{3}{2}h_1h_2^2 + \frac{3}{4}h_1^2h_2\right) + \frac{c_{33p}^3}{3}\left(h_3^3 + \frac{3}{2}h_1h_3^2 + \frac{3}{4}h_1^2h_3\right)$$

$$D_2 = \frac{1}{12}c_{13p}^1 h_1^3 + \frac{c_{13p}^2}{3}\left(h_2^3 + \frac{3}{2}h_1h_2^2 + \frac{3}{4}h_1^2h_2\right) + \frac{c_{13p}^3}{3}\left(h_3^3 + \frac{3}{2}h_1h_3^2 + \frac{3}{4}h_1^2h_3\right)$$

$$D_3 = A_3, \quad D_4 = A_4, \quad D_5 = \frac{e_{33p}^2}{2}(h_1h_2 + h_2^2) - \frac{e_{33p}^2}{2}(h_1h_3 + h_3^2)$$

$$D_6 = -\frac{\lambda_2^2}{2}(h_1h_2 + h_2^2) + \frac{\lambda_2^3}{2}(h_1h_3 + h_3^2)$$

$$E_1 = \frac{1}{12}c_{11p}^1 h_1^3 + \frac{c_{11p}^2}{3}\left(h_2^3 + \frac{3}{2}h_1h_2^2 + \frac{3}{4}h_1^2h_2\right) + \frac{c_{11p}^3}{3}\left(h_3^3 + \frac{3}{2}h_1h_3^2 + \frac{3}{4}h_1^2h_3\right)$$

$$E_2 = D_2, \quad E_3 = B_3, \quad E_4 = A_4, \quad E_5 = \frac{e_{31p}^2}{2}(h_1h_2 + h_2^2) - \frac{e_{31p}^3}{2}(h_1h_3 + h_3^2)$$

$$E_6 = -\frac{\lambda_1^2}{2}(h_1h_2 + h_2^2) + \frac{\lambda_1^3}{2}(h_1h_3 + h_3^2)$$

$$F_1 = \frac{1}{12}c_{44p}^1 h_1^3 + \frac{c_{44p}^2}{3}\left(h_2^3 + \frac{3}{2}h_1h_2^2 + \frac{3}{4}h_1^2h_2\right) + \frac{c_{44p}^3}{3}\left(h_3^3 + \frac{3}{2}h_1h_3^2 + \frac{3}{4}h_1^2h_3\right)$$

$$F_2 = C_2, \quad F_3 = \frac{e_{15p}^2}{2}(h_1h_2 + h_2^2) - \frac{e_{15p}^3}{2}(h_1h_3 + h_3^2)$$

Appendix B

$$a_{11} = -A_1\xi^2 - \frac{n^2}{R}C_1 + (\rho_1h_1 + \rho_2h_2 + \rho_3h_3)\omega^2, \quad a_{12} = in\xi\left(\frac{A_2}{R} + \frac{C_1}{R}\right), \quad a_{13} = i\xi\frac{A_2}{R}$$

$$a_{14} = -A_3\xi^2 - \frac{C_2}{R^2}n^2 + \frac{\omega^2}{R}\left[\frac{\rho_1h_1^3}{12} + \frac{\rho_2}{3}\left(h_2^3 + \frac{3}{2}h_1h_2^2 + \frac{3}{4}h_1^2h_2\right) + \frac{\rho_3}{3}\left(h_3^3 + \frac{3}{2}h_1h_3^2 + \frac{3}{4}h_1^2h_3\right)\right]$$

$$a_{15} = in\xi\left(\frac{A_4}{R} + \frac{C_2}{R}\right), \quad a_{16} = -A_5\xi^2 - \frac{C_3}{R^2}n^2, \quad a_{17} = i\xi(-\lambda_2^1h_1 - \lambda_2^2h_2 - \lambda_2^3h_3), \quad a_{21} = -a_{12}$$

$$a_{22} = -\frac{B_1}{R^2}n^2 - C_1\xi^2 - \frac{k}{R^2}(c_{44p}^1h_1 + c_{44p}^2h_2 + c_{44p}^3h_3) + (\rho_1h_1 + \rho_2h_2 + \rho_3h_3)\omega^2$$

$$a_{23} = -\frac{B_1}{R^2}n - \frac{kn}{R^2}(c_{44p}^1h_1 + c_{44p}^2h_2 + c_{44p}^3h_3), \quad a_{24} = -in\xi\left(\frac{B_4}{R} + \frac{C_2}{R}\right)$$

$$a_{25} = -C_2\xi^2 - \frac{B_3}{R^2}n^2 + \frac{k}{R}(c_{44p}^1h_1 + c_{44p}^2h_2 + c_{44p}^3h_3)$$
$$+ \frac{\omega^2}{R}\left[\frac{\rho_1h_1^3}{12} + \frac{\rho_2}{3}\left(h_2^3 + \frac{3}{2}h_1h_2^2 + \frac{3}{4}h_1^2h_2\right) + \frac{\rho_3}{3}\left(h_3^3 + \frac{3}{2}h_1h_3^2 + \frac{3}{4}h_1^2h_3\right)\right]$$

$$a_{26} = -in\xi\Big(\frac{B_5}{R} + \frac{C_3}{R}\Big), \quad a_{27} = -\frac{n}{R}i\xi(-\lambda_1^1 h_1 - \lambda_1^2 h_2 - \lambda_1^3 h_3), \quad a_{31} = -a_{13}, \quad a_{32} = a_{23}$$

$$a_{33} = k(c_{44p}^1 h_1 + c_{44p}^2 h_2 + c_{44p}^3 h_3)\Big(-\xi^2 - \frac{n^2}{R^2}\Big) - \frac{B_1}{R^2}(\rho_1 h_1 + \rho_2 h_2 + \rho_3 h_3)\omega^2$$

$$a_{34} = i\xi\Big(k(c_{44p}^1 h_1 + c_{44p}^2 h_2 + c_{44p}^3 h_3) - \frac{B_4}{R}\Big), \quad a_{35} = \frac{kn}{R^2}(c_{44p}^1 h_1 + c_{44p}^2 h_2 + c_{44p}^3 h_3) - \frac{B_3}{R^2}n$$

$$a_{36} = -i\xi\frac{B_5}{R}, \quad a_{37} = -\frac{1}{R}(-\lambda_1^1 h_1 - \lambda_1^2 h_2 - \lambda_1^3 h_3), \quad a_{41} = a_{14}, \quad a_{42} = -a_{24}, \quad a_{43} = -a_{34}$$

$$a_{44} = -D_1\xi^2 - \frac{F_1}{R^2}n^2 - k(c_{44p}^1 h_1 + c_{44p}^2 h_2 + c_{44p}^3 h_3)$$

$$+ \omega^2\Big[\frac{\rho_1 h_1^3}{12} + \frac{\rho_2}{3}\Big(h_2^3 + \frac{3}{2}h_1 h_2^2 + \frac{3}{4}h_1^2 h_2\Big) + \frac{\rho_3}{3}\Big(h_3^3 + \frac{3}{2}h_1 h_3^2 + \frac{3}{4}h_1^2 h_3\Big)\Big]$$

$$a_{45} = in\xi\Big(\frac{D_2}{R} + \frac{F_1}{R}\Big), \quad a_{46} = -\frac{F_3}{R^2}n^2 - D_5\xi^2, \quad a_{47} = i\xi\Big(-\frac{\lambda_2^2}{2}(h_1 h_2 + h_2^2) + \frac{\lambda_2^3}{2}(h_1 h_3 + h_3^2)\Big), \quad a_{51} = -a_{15}$$

$$a_{52} = a_{25}, \quad a_{53} = a_{35}, \quad a_{54} = -a_{45}$$

$$a_{55} = -F_1\xi^2 - \frac{E_1}{R^2}n^2 - k(c_{44p}^1 h_1 + c_{44p}^2 h_2 + c_{44p}^3 h_3)$$

$$+ \omega^2\Big[\frac{\rho_1 h_1^3}{12} + \frac{\rho_2}{3}\Big(h_2^3 + \frac{3}{2}h_1 h_2^2 + \frac{3}{4}h_1^2 h_2\Big) + \frac{\rho_3}{3}\Big(h_3^3 + \frac{3}{2}h_1 h_3^2 + \frac{3}{4}h_1^2 h_3\Big)\Big]$$

$$a_{56} = -in\xi\Big(\frac{E_5}{R} + \frac{F_3}{R}\Big), \quad a_{57} = -\frac{n}{R}\Big(-\frac{\lambda_1^2}{2}(h_1 h_2 + h_2^2) + \frac{\lambda_1^3}{2}(h_1 h_3 + h_3^2)\Big)$$

$$a_{61} = -e_{33p}^2\xi^2 - \frac{e_{15p}^2}{R^2}n^2, \quad a_{62} = \frac{i\xi n}{R}(e_{31p}^2 + e_{15p}^2), \quad a_{63} = \frac{ie_{31p}^1\xi}{R}$$

$$a_{64} = -\frac{e_{33p}^2}{2}(h_1 + h_2)\xi^2 - \frac{e_{15p}^2}{2R^2}(h_1 + h_2)n^2$$

$$a_{65} = i\xi n\Big[\frac{e_{33p}^2}{2R}(h_1 + h_2)\xi^2 + \frac{e_{15p}^2}{2R}(h_1 + h_2)\Big], \quad a_{66} = \Xi_{33p}^2\xi^2 + \frac{1}{R^2}\Xi_{11p}^2 n^2, \quad a_{67} = ip_3^2\xi$$

$$a_{71} = -e_{33p}^3\xi^2 - \frac{e_{15p}^3}{R^2}n^2, \quad a_{72} = \frac{i\xi n}{R}(e_{31p}^3 + e_{15p}^3), \quad a_{73} = \frac{ie_{31p}^3\xi}{R}$$

$$a_{74} = \frac{e_{33p}^3}{2}(h_1 + h_2)\xi^2 + \frac{e_{15p}^3}{2R^2}(h_1 + h_2)n^2, \quad a_{75} = -i\xi n\Big(\frac{e_{33p}^3}{2R}(h_1 + h_2)\xi^2 + \frac{e_{15p}^3}{2R}(h_1 + h_2)\Big)$$

$$a_{76} = \Xi_{33p}^3\xi^2 + \frac{1}{R^2}\Xi_{11p}^3 n^2, \quad a_{77} = ip_3^3\xi$$

Appendix C

Table 1 Materials properties of laminated piezoelectric cylindrical shells

Properties	PVDF	Al	T700/Epoxy	PZT-4
Mass density (kg/m^3)	1.8×10^3	2.8×10^3	1.5×10^3	7.5×10^3
c_{11} (GPa)	3.61	105	148	132
c_{12}	1.61	51	4.8	71
c_{13}	1.42	51	4.8	73
c_{33}	1.63	105	12	115
c_{44}	0.55	105	5	26
c_{55}	0.59	105	5	26
e_{31} (k/m^2)	32.075×10^{-3}	-	-	-4.1
e_{33}	-21.19×10^{-3}	-	-	14.1
e_{15}	-15.93×10^{-3}	-	-	10.5
Ξ_{11} (ϕ/m)	53.985×10^{-12}	-	-	5.841×10^{-9}
Ξ_{33}	59.295×10^{-12}	-	-	7.124×10^{-9}
Thermal expansion coefficient (/ ^{o}C)				
α_{11}	1.2×10^{-4}	2.55×10^{-5}	0.02×10^{-6}	1.2×10^{-6}
α_{22}	1.2×10^{-4}	2.55×10^{-5}	22.5×10^{-6}	1.2×10^{-6}
Pyroelectric constant				
p	-4×10^{-5}	-	-	0.25×10^{-4}
Humidity expansion coefficient (wt.%H_2O)$^{-1}$				
η_{11}	-	-	0.005×10^{-6}	-
η_{22}	-	-	0.6×10^{-6}	-